

SoundMorpher: Perceptually-Uniform Sound Morphing with Diffusion Model

Xinlei Niu, *Member, IEEE*, Jing Zhang, *Member, IEEE*, and Charles Patrick Martin, *Member, IEEE*

Abstract—We present SoundMorpher, an open-world sound morphing method designed to generate perceptually uniform morphing trajectories. Traditional sound morphing techniques typically assume a linear relationship between the morphing factor and sound perception, achieving smooth transitions by linearly interpolating the semantic features of source and target sounds while gradually adjusting the morphing factor. However, these methods oversimplify the complexities of sound perception, resulting in limitations in morphing quality. In contrast, SoundMorpher explores an explicit relationship between the morphing factor and the perception of morphed sounds, leveraging log Mel-spectrogram features. This approach further refines the morphing sequence by ensuring a constant target perceptual difference for each transition and determining the corresponding morphing factors using binary search. To address the lack of a formal quantitative evaluation framework for sound morphing, we propose a set of metrics based on three established objective criteria. These metrics enable comprehensive assessment of morphed results and facilitate direct comparisons between methods, fostering advancements in sound morphing research. Extensive experiments demonstrate the effectiveness and versatility of SoundMorpher in real-world scenarios, showcasing its potential in applications such as creative music composition, film post-production, and interactive audio technologies.

Index Terms—Sound morphing, open-world, diffusion models.

I. INTRODUCTION

SOUND morphing is a technique to create a seamless transformation between multiple sound recordings. The goal is to produce intermediate sounds that might exist between two sounds and contrasts with simpler mixing or cross-fading between sounds. Sound morphing has a wide range of applications, including music compositions, synthesizers, psychoacoustic experiments to study timbre spaces [1], [2], film post-production, AR/VR, and adaptive audio content in video games [3], [4]. Traditionally, sound morphing relied on interpolating the parameters of a sinusoidal synthesis model [5]–[7]. High-level audio features in the time-frequency domain can also be controlled to achieve more effective and continuous morphing [1], [7]–[11]. These techniques have quality limitations that rule out applications in inharmonic and noisy sounds such as environmental sounds [12], [13]. Increasing interest in sound generation using machine learning (ML) has delivered techniques for ML-based sound morphing [12]–[15] that out-perform traditional methods in scenarios such as timbre morphing, audio texture morphing and environmental

sound morphing; however, we observed critical limitations of these existing sound morphing methods. Firstly, they are primarily designed for specific morphing methods or tailored to particular application scenarios on task-specific datasets, which limits their ability to broader applications and different scenarios. Secondly, a lack of sufficient and formal quantitative evaluation limits further analysis of their effectiveness [12] and impedes fair comparisons with other sound morphing techniques. Most importantly, these methods typically assume a linear relationship between morphing factors and sound perception, as proposed by [16]. They achieve smooth morphing by interpolating semantic features linearly between the source and target sounds and gradually varying the morphing factor. This assumption oversimplifies the complex nature of sound perception, as gradually changing morph factors does not inherently result in smooth perceptual transitions. Our goal is to address these limitations by introducing SoundMorpher, a *flexible sound morphing method*, which can be broadly applied to different sound morphing tasks to achieve perceptually coherent morph, ensuring seamless and natural sound transition. In this work we:

- Introduce the first open-world sound morphing method based on a pre-trained diffusion model, which integrates typical morph tasks such as static, dynamic and cyclo-stationary morphing. Unlike [12], [15], SoundMorpher can be broadly applied to various real-world sound morphing tasks without requiring extensive retraining on an additional dataset, paving the way for future sound morphing studies to focus on leveraging pre-trained audio generation models for greater efficiency and versatility.
- Propose sound perceptual distance proportion (SPDP), which explicitly connects morph factors and perception of morphed results. This allows SoundMorpher to produce morphing paths with a uniform change in perceptual stimuli, achieving more seamless perceptual transitions compared to existing methods [13].
- Adapt established criteria [16] for quantitative evaluation, addressing the lack of comprehensive objective quantitative assessment for sound morphing systems [11], [14], [17].
- Provide extensive experiments to demonstrate that SoundMorpher can be effectively applied to various applications in real-world scenarios including timbre morphing, music morphing and environmental sound morphing.

Our demonstration and codes are available at <https://xinleiniu.github.io/SoundMorpher-demo/>

II. RELATED WORK

In this section, we present a detailed review of related works on sound morphing task and briefly introduce contrasts with other similar tasks.

Sound morphing. Traditional sound morphing methods are based on interpolating parameters of a sinusoidal sound synthesis model [5]–[7], [18]. To achieve more effective and continuous morphing, [1], [7]–[10], [19] exploring perceptual spectral domain audio features by digital signal processing techniques, such as MFCCs, spectral envelope, etc. A hybrid approach has been explored that extracts audio descriptors to morph accordingly and interpolates between the spectrotemporal fine structures of two endpoints according to morph factors [20]. Machine learning sound morphing methods offer advantages such as high morphing quality by interpolation of semantic representations within a model instead of traditional audio features. [14] proposes a non-parallel many-to-one static timbre morphing framework that integrates and fine-tunes the machine learning technique (i.e., DDSP-autoencoder [21]) with spectral feature interpolation [17]. [15] synthesizes music corresponding to a note sequence and timbre, using nonlinear instrument embeddings as timbre control parameters under a pretrained WaveNet [22] to achieve timbre morphing between instruments. [23] learns latent distributions of VAEs to disentangle representations of the pitch and timbre of musical instrument sounds. [24] uses a GM-VAE to achieve style morphing to generate realistic piano performances in the audio domain following temporal style conditions for piano performances, which morphs the conditions such as onset roll and MIDI note into input audio. MorphGAN [12] targets audio texture morphing by interpolating within conditional parameters training the model on a water-wind texture dataset. A recent concurrent work [13] uses a pre-trained AudioLDM [25] to morph sound between two text prompts. In contrast, we focus on classical sound morphing, where the morphing process is performed directly between two given sounds rather than between text prompts. A key advantage of our method is its ability to provide precise guidance during the morphing process, since the target audio delivers exact information on how the source sound should evolve—something that text prompts cannot always achieve, for example, morphing between two music compositions.

Synthesizer preset interpolation. A form of sound morphing can be achieved by developing models that compute interpolations in the parameters for a black-box synthesizer [26]–[28]. Unlike classical sound morphing, which perceptually blends two audio files into an intermediate sound, synthesizer preset interpolation treats the synthesizer as a non-differentiable black box, with presets composed of both numerical and categorical parameters. By smoothly interpolating between these presets, the task aims to achieve seamless morphing of synthesized sounds.

Text-to-audio editing. Text-to-audio editing is the process of using text queries to edit audio. With the success of diffusion models in image editing tasks, recent works target zero-shot audio editing with text instructions [29]–[31] involving tasks such as inpainting, outpainting, timbre transfer, music

genre transfer, or vocals removal.

Timbre transfer. Timbre transfer is a specific task that aims at converting the sound of a musical piece by one instrument (source) into the same piece played by another instrument (target). This concerns the task of converting a musical piece from one timbre to another while preserving the other music-related characteristics [32]–[34].

Voice conversion and morphing. Voice conversion (VC) involves modifying vocal characteristics of a source speech to match a target speaker, either by using target speeches or text [35]–[38]. The primary objective of VC is to alter the vocal identity to closely resemble the target voice style while preserving the linguistic content of the source speech. Voice morphing is a broader scope, focusing on blending or transforming one voice into another. This often involves creating an intermediate voice that incorporates characteristics of both source and target voices, allowing for gradual transitions between them [38].

III. PRELIMINARIES

A. Sound Morphing

Sound morphing aims to produce intermediate sounds as different combinations of model source sound \hat{S}_1 and target sound \hat{S}_2 [1], [9], which can be formulated as

$$M(\alpha, t) = (1 - \alpha(t))\hat{S}_1 + \alpha(t)\hat{S}_2 \quad (1)$$

Each step is characterized by one value of a single parameter α , the so-called morph factor, which ranges between 0 and 1. $\alpha = 0$ and $\alpha = 1$ produce resynthesized source and target sounds, respectively. Due to the intrinsic temporal nature of sounds, sound morphing usually involves three main types: *dynamic morphing*, where α gradually transfers from 0 to 1 over time [20], *static morphing*, where a single morph factor α leads to an intermediate sound between source and target [39], and *cyclostationary morphing* where several hybrid sounds are produced in different intermediate points [40].

To solve the limitation on previous works that target on expensive perceptual evaluation only, [16] provided three objective criteria to formalize the evaluation for sound morphing methods: (1) *Correspondence*. The morph is achieved by a description whose elements are intermediate between source and target sounds, highlighting semantic level transition; (2) *Intermediateness*. The morphed objects should be perceived as intermediate between source and target sounds, evaluating perceptual level correlation; (3) *Smoothness*. The morphed sounds should change gradually from source to target sounds, by the same amount of perception increment. Specifically, the linear assumption proposed by [16] is that adding the same amount of morph factor should increase the same amount of perception difference.

In this study, we evaluate SoundMorpher according to the three criteria proposed by [16] with a series of comprehensive objective quantitative metrics.

B. Latent Diffusion Model on Audio Generation

SoundMorpher uses a pretrained text-to-audio (TTA) latent diffusion model (LDM) [41] to achieve sound morphing. This

approach offers the advantage of performing various types of sound morphing without the need to train the entire model or use additional datasets. Specifically, we use AudioLDM2 [42], a multi-modality conditions to audio model. It employs a pre-trained variational autoencoder (VAE) [43] to compress audio x into a low-dimension latent space as VAE representations z . AudioLDM2 generates latent variables z_0 from a Gaussian noise z_T given the condition C and further reconstructs audio \hat{x} from z_0 by VAE decoder and a vocoder [44]. AudioLDM2 uses an intermediate feature Y as an abstraction of audio data x to bridge the gap between conditions C and audio x , named language of audio (LOA). The LOA feature is obtained by a AudioMAE [45], [46] and a series of post-processing formulated as $Y = \mathcal{A}(x)$. The generation function $\mathcal{G}(\cdot)$ is achieved by a LDM. In the inference phase, AudioLDM2 approximates LOA feature by the given condition as $\hat{Y} = \mathcal{M}(C)$ using a fine-tuned GPT-2 model [47]. Then generates audios conditioned on the estimated LOA feature \hat{Y} and an extra text embedding E_{T5} from a FLAN-T5 [48] with a LDM as $\hat{x} = \mathcal{G}(\hat{Y}, E_{T5})$. We denote the conditional embeddings in AudioLDM2 as $E = \{\hat{Y}, E_{T5}\}$, therefore, the generative process becomes $\hat{x} = \mathcal{G}(E)$.

Diffusion Models. The LDM performs a forward diffusion process during training, which is defined as a Markov chain that gradually adds noise to the VAE representation z_0 over T steps as $z_t = \sqrt{1 - \beta_t}z_{t-1} + \sqrt{\beta_t}\epsilon_t$, where $\epsilon_t \sim N(0, I)$ and noise schedule hyperparameter $\beta_t \in [0, 1]$. Therefore, we can derive the distribution of z_t given z_0 as $q(z_t|z_0) = \sqrt{\gamma_t}z_0 + \sqrt{1 - \gamma_t}\epsilon_t$, where $\gamma_t = \prod_{s=1}^t 1 - \beta_s$. The LDM learns a backward transition $\epsilon_\theta(z_t, t)$ from the prior distribution $N(0, I)$ to the data distribution z , that predicts the added noise ϵ_t [49]. Following the objective function of denoising diffusion probabilistic models (DDPM) [49], the objective function for training AudioLDM2 is

$$\min_{\theta} \mathcal{L}_{\text{DPM}} = \min_{\theta} [\mathbb{E}_{z_0, E, t \sim \{1, \dots, T\}} \|\epsilon_\theta(z_t, E, t) - \epsilon_t\|_2^2] \quad (2)$$

To reduce computational demands on inference, AudioLDM2 uses denoising diffusion explicit models (DDIM) [50], which provides an alternative solution and enables significantly reduced sampling steps with high generation quality. We can revise a deterministic mapping between z_0 and its latent STATE z_T once the model is trained [51], [52] by the equation

$$\frac{z_{t+1}}{\sqrt{\gamma_{t+1}}} - \frac{z_t}{\sqrt{\gamma_t}} = \left(\sqrt{\frac{1 - \gamma_{t+1}}{\gamma_{t+1}}} - \sqrt{\frac{1 - \gamma_t}{\gamma_t}} \right) \epsilon_\theta(z_t, E, t) \quad (3)$$

IV. METHOD

Given a source and target audio pair $\{x^{(0)}, x^{(1)}\}$, sound morphing aims to generate intermediate sounds $x^{(\alpha(t))}$ between the audio pair given morph factors $\alpha \in [0, 1]$. To account for the variation of α over time in Equation 1, we discretize the function $\alpha(t)$ where $t \in [0, T]$ into N elements, resulting in a morphed sequence of sounds $\{x^{(\alpha_i)}\}_{i=1}^N$ based on $\{\alpha_i\}_{i=1}^N$. According to the smoothness criteria proposed by [16], a desired sound morphing results should exhibit a *linear perceptual change* as the morph factor α transitions

through the sequence $\alpha_{i=1}^N$. Therefore, we define p_i to represent the perception of the morphed audio $x^{(\alpha_i)}$ given morph factor α_i . However, the relationship $\mathcal{P}(\cdot)$ between morph factor α and perceptual stimuli p is intractable. Our objective is to determine a discrete sequence of morph factors $\{\alpha_i\}_{i=1}^N$ such that the perceptual stimulus difference Δp remains constant for each transition. We formulate the problem as

$$p_{i+1} - p_i \equiv \mathcal{P}(x^{(\alpha_{i+1})}) - \mathcal{P}(x^{(\alpha_i)}) = \Delta p \quad (4)$$

where $i \in [1, \dots, N - 1]$.

This formulation is a refined sound morphing problem where, rather than controlling morph factor α , we control the constant perception difference Δp to find the optimal trajectory with morph factors $\{\alpha_i\}_{i=1}^N$ that will achieve *perceptually uniform sound morphing*. The overall pipeline of SoundMorpher is presented in Fig. 1 and Algorithm 1.

In Section IV-A and Section IV-B, we introduce feature interpolation and model adaptation with a pre-trained AudioLDM2. This method allows high-quality intermediate morph results to be obtained by interpolating semantic conditional embeddings of source and target sounds according to morph factor α . In Section IV-C, we explore an explicit connection $\mathcal{P}(\cdot)$ between perceptual stimuli p and morph factor α to achieve perceptually uniform sound morphing, as in Equation 4. This approach enables us to refine the morph factors using binary search to achieve the desired perceptual differences Δp for each transition. In Section IV-D, we provide extensions of our method on the different morphing methods discussed in Section III-A to show the advantages of perceptually uniform sound morphing.

A. Feature Interpolation

Similar to other sound morphing methods, SoundMorpher achieves sound morphing by interpolating features between source and target audios. In this section, we introduce a method to bridge the source and target audios based on semantic conditional embeddings in a pre-trained AudioLDM2, leading to a controllable sound morphing method by a morph factor α .

Interpolating optimized conditional embeddings. We first introduce a text-guided conditional embedding optimization strategy under a pre-trained AudioLDM2 [42], which retrieves corresponding conditional embeddings E of the given audio data. This optimization strategy enables our sound morphing method to handle diverse types of sounds without requiring the model to be retrained on specific datasets. As mentioned in Section III-B, AudioLDM2 accepts two conditional inputs: LOA feature Y and text embedding E_{T5} . We denote $E = \{Y, E_{T5}\}$ as the overall conditional embedding inputs for AudioLDM2. The LOA feature Y is an abstraction of audio data which is semantically structured, and E_{T5} captures sentence-level of representations.

$$\begin{aligned} E^{(0)} &= \min_E \mathcal{L}_{\text{DPM}}(z_0^{(0)}, E; \theta) \text{ and} \\ E^{(1)} &= \min_E \mathcal{L}_{\text{DPM}}(z_0^{(1)}, E; \theta) \end{aligned} \quad (5)$$

The optimized conditional embeddings $E^{(0)}$ and $E^{(1)}$ fully encapsulate the abstract details of audios $x^{(0)}$ and $x^{(1)}$. Due to

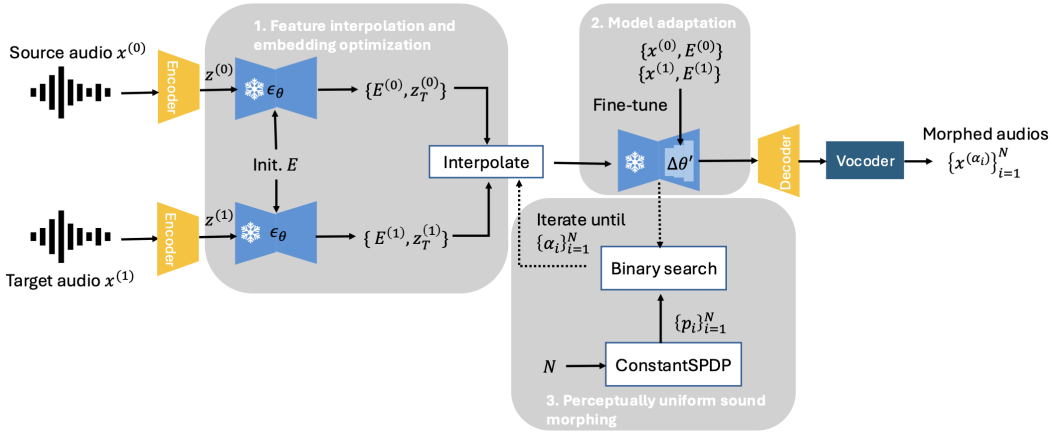


Fig. 1. Overview of SoundMorpher pipeline, where the snowflake represents the model parameters are frozen.

the semantically structured nature of the conditional embeddings, the conditional distributions $p_\theta(z|E^{(0)})$ and $p_\theta(z|E^{(1)})$ closely mirror the degree of audio variation between the audio pair. To explore the data distribution that conceptually intermediate between $z^{(0)}$ and $z^{(1)}$, we bridge these two distributions through linear interpolation. Specifically, we define the interpolated conditional distribution as $p_\theta(z|E^{(\alpha)}) := p_\theta(z|(1-\alpha)E^{(0)} + \alpha E^{(1)})$, where $\alpha \in [0, 1]$.

Interpolating latent state. The conditional embedding represents the conceptual abstract of audio. We also wish to smoothly morph the content of the audio pair. Following [50], we smoothly interpolate between $z_0^{(0)}$ and $z_0^{(1)}$ by spherical linear interpolation (slerp) to their starting noise $z_T^{(0)}$ and $z_T^{(1)}$ and further obtained the interpolated latent state $z_T^{(\alpha)} := \frac{\sin((1-\alpha)\omega)}{\sin\omega} z_T^{(0)} + \frac{\sin\alpha\omega}{\sin\omega} z_T^{(1)}$, where $\omega = \arccos(\frac{z_T^{(0)\top} z_T^{(1)}}{\|z_T^{(0)}\| \|z_T^{(1)}\|})$. The denoised latent variable $z_0^{(\alpha)}$ is obtained by applying a diffusion denoising process on the interpolated starting noise $z_T^{(\alpha)}$ and conditioning on the interpolated conditional embedding $E^{(\alpha)}$. The final morphed audio result $x^{(\alpha)}$ is obtained from $z_0^{(\alpha)}$ by the VAE decoder and a vocoder.

B. Model adaptation

Model adaptation helps to limit the degree of morphed variation by suppressing high-density regions that not related to the given inputs [52]. To enhance the output quality of source and target audios. We follow [52] and use LoRA [53] to inject a small amount of trainable parameters for efficient model adaptation. We fine-tune AudioLDM2 with LoRA trainable parameters using $z^{(0)}$ and $z^{(1)}$. Compared to vanilla fine-tuning approaches, LoRA has advantages in training efficiency with injecting small amount of trainable parameters. The model adaptation can be defined as

$$\begin{aligned} & \min_{\Delta\theta'} \mathcal{L}_{\text{DPM}}(z_0^{(0)}, E^{(0)}; \theta + \Delta\theta') + \\ & \min_{\Delta\theta'} \mathcal{L}_{\text{DPM}}(z_0^{(1)}, E^{(1)}; \theta + \Delta\theta') \text{ s.t. } \text{rank}(\Delta\theta') = r \end{aligned} \quad (6)$$

where r represents LoRA rank.

To achieve high text alignment on inference, we use another LoRA parameters $\Delta\theta_0$ with rank r_0 to perform bias correction

$$\begin{aligned} & \min_{\Delta\theta_0} \mathcal{L}_{\text{DPM}}(z_0^{(0)}, \emptyset; \theta + \Delta\theta_0) + \\ & \min_{\Delta\theta_0} \mathcal{L}_{\text{DPM}}(z_0^{(1)}, \emptyset; \theta + \Delta\theta_0) \text{ s.t. } \text{rank}(\Delta\theta_0) = r_0 \end{aligned} \quad (7)$$

During inference, with $\theta' = \theta + \Delta\theta'$ and $\theta_0 = \theta + \Delta\theta_0$, the noise prediction becomes

$$\hat{\epsilon}_\theta(z_t, t, E) := w\epsilon_{\theta'}(z_t, t, E) + (1-w)\epsilon_{\theta_0}(z_t, t, \emptyset). \quad (8)$$

Although [52] provide a heuristic suggestion for setting the LoRA rank value in the image morphing task; however, we further investigate the relationship between LoRA rank r and method performance in our empirical experiment.

C. Perceptually Uniform Sound Morphing

Although interpolating semantic features between the source and target audios enables a smooth transition by leveraging the inherent structure of the semantic space, our ultimate goal is to explore the complex relationship between sound perception and the morph factor to further enhance the smoothness of the morphing sequence. In this section, we propose a method to further refine the morphed results by fixing the perception difference for each transition as constant as in Equation 4. **Sound perceptual distance proportion (SPDP).** The relationship between morph factor α and perceptual stimuli p is intractable. Our goal is to establish an objective quantitative metric that links p_i and $x^{(\alpha_i)}$ as in Equation 4. This metric should satisfy two key conditions: (1) the output p should increase monotonically as α increases; (2) it should accurately represent sound perception and audio descriptive difference between $x^{(\alpha)}$ and $\{x^{(0)}, x^{(1)}\}$, ensuring a smooth transition through intermediate states.

To this end, we propose the *sound perceptual distance proportion* between $x^{(\alpha)}$ and $\{x^{(0)}, x^{(1)}\}$. We define $p_i \in \mathbb{R}^2$ as a 2D vector to represent the perceptual proximity of $x^{(\alpha_i)}$ to both $x^{(0)}$ and $x^{(1)}$. Instead of extracting numerous audio features through traditional signal processing techniques, we use log magnitude Mel-scaled spectrogram to capture *perceptual information* and *descriptive aspects* of audio, aligning well with the three objective criteria outlined in Section III-A.

Algorithm 1 Overall pipeline of SoundMorpher

Require: A pre-trained AudioLDM2 pipeline including a pre-trained VAE with an encoder g_θ and a decoder g_ϕ , a pre-trained latent diffusion model ϵ_θ , a pre-trained T5 model f_ϕ , and a pre-trained GPT-2 model f_φ . Learning rates η_1, η_2 . Source and target audios $x^{(0)}$ and $x^{(1)}$. An initial text prompts y . perceptually uniform interpolation number N . tolerance error for binary search ϵ_{tol} . Number of training steps for text inversion for conditional embedding optimization T_{inv} . Number of training steps for model adaptation T_{adapt} . LoRA rank r , step number of DDIM T .

Ensure: Start morph factor $\alpha_{start} = 0$, end morph factor $\alpha_{end} = 1$. Start perceptual point $p_{start} = [0, 1]$, and end perceptual point $p_{end} = [1, 0]$.

Initialize: $z_0^{(0)} = g_\theta(x_0^{(0)})$, $z_0^{(1)} = g_\theta(x_0^{(1)})$; $E^0 = [f_\phi(y), f_\varphi(y)]$, $E^1 = [f_\phi(y), f_\varphi(y)]$;

Step 1: Text-guided conditional embedding optimization
for i **from** 1 **to** T_{inv} **do**

Randomly sample time step t and random noise $\epsilon_t \sim N(0, I)$.

Adding noise to data $z_t^{(0)} \leftarrow \sqrt{\gamma_t}z_0^{(0)} + \sqrt{(1-\gamma_t)}\epsilon_t$,

$z_t^{(1)} \leftarrow \sqrt{\gamma_t}z_0^{(1)} + \sqrt{(1-\gamma_t)}\epsilon_t$.

$E^{(0)} \leftarrow E^{(0)} - \eta_1 \nabla_{E^{(0)}} \mathcal{L}_{DPM}(z_0^{(0)}, E^{(0)}; \theta)$.

$E^{(1)} \leftarrow E^{(1)} - \eta_1 \nabla_{E^{(1)}} \mathcal{L}_{DPM}(z_0^{(1)}, E^{(1)}; \theta)$.

end for

Step 2: Model adaptation with LoRA.

for i **from** 1 **to** T_{adapt} **do**

Model adaptation with LoRA according to Equation 6 and Equation 7 with η_2 learning rate.

end for

Step 3: Perceptual-uniform binary search with constant SPDP increment

Obtaining initial latent states $z_T^{(0)}$ and $z_T^{(1)}$ by Equation 3

$p_{list} \leftarrow \text{ConstantSPDP}(N, p_{start}, p_{end})$

$\alpha_{list} \leftarrow \text{BinarySeach}(\alpha_{start}, \alpha_{end}, p_{list}, \epsilon_{tol})$

Interpolate embeddings and latent state

for α **in** α_{list} **do**

$E^{(\alpha)} \leftarrow (1-\alpha)E^{(0)} + \alpha E^{(1)}$

$z_T^{(\alpha)} \leftarrow \frac{\sin((1-\alpha)w)}{\sin w} z_T^{(0)} + \frac{\sin \alpha w}{\sin w} z_T^{(1)}$

for t **from** T **to** 1 **do**

$z_{t-1}^{(\alpha)} \leftarrow \sqrt{\gamma_{t-1}} \left(\frac{z_t - \sqrt{1-\gamma_t} \hat{\epsilon}_\theta^{(t)}(z_t, E^{(\alpha)})}{\sqrt{\gamma_t}} \right) +$

$\sqrt{1-\gamma_{t-1}} \hat{\epsilon}_\theta^{(t)}(z_t, E^{(\alpha)})$

end for

end for

$x^{(\alpha)} \leftarrow \text{vocoder}(g_\phi(z_0^{(\alpha)}))$

return $\{x^{(\alpha)}\}_{\alpha \in \alpha_{list}}$

The log Mel-spectrogram [54] provides a pseudo-3D representation of audio signals, with one axis representing time and the other representing frequency on the Mel scale [55], while the values denote the magnitude of each frequency at specific time points. This visual representation enables humans to intuitively interpret audio characteristics and descriptive information through its structured depiction of temporal and spectral features. Another advantage of using Mel-spectrogram

lies in the Mel filter banks, which map frequencies to equal pitch distances that correspond to how humans perceive sound [56], [57]. A logarithmic scaling on the frequency further addresses the imbalance in human perception, which is inherently logarithmic and tends to disproportionately affect low and high-frequency regions. This approach aligns with the principles of psychoacoustics, which suggest that human auditory perception is better represented on a logarithmic frequency scale [58], [59].

Denoting $x_{mel}^{(\alpha_i)}$ as the log magnitude Mel-spectrogram of audio $x^{(\alpha_i)}$, the SPDP point p_i of $x^{(\alpha_i)}$ between $x^{(0)}$ and $x^{(1)}$ given α_i is defined as

$$p_i = \left[\frac{\|x_{mel}^{(\alpha_i)} - x_{mel}^{(0)}\|_2}{\|x_{mel}^{(\alpha_i)} - x_{mel}^{(0)}\|_2 + \|x_{mel}^{(\alpha_i)} - x_{mel}^{(1)}\|_2}, \quad (9) \right. \\ \left. \frac{\|x_{mel}^{(\alpha_i)} - x_{mel}^{(1)}\|_2}{\|x_{mel}^{(\alpha_i)} - x_{mel}^{(0)}\|_2 + \|x_{mel}^{(\alpha_i)} - x_{mel}^{(1)}\|_2} \right]$$

Equation 9 calculates the distance proportion of how the morphed sample $x^{(\alpha_i)}$ closes between source $x^{(0)}$ and target $x^{(1)}$, meanwhile the L2 norm measures the distance between two log Mel spectrograms. Therefore, the summation of the two elements in p are always equals to 1. Furthermore, the first element of p_i is strictly monotonically increasing with α while the second element is strictly monotonically decreasing, providing a clear and interpretable relationship between the parameter α and the perceptual proximity of $x^{(\alpha_i)}$ to $x^{(0)}$ and $x^{(1)}$. In summary, the log Mel-spectrogram effectively captures both perceptual and descriptive audio information, offering an elegant solution to satisfy the criterions of smoothness, correspondence, and intermediateness proposed by [16].

Binary search with constant SPDP increment. To produce a perceptually smooth morphing trajectory with a constant perceptual stimuli increment, we use binary search to search for the corresponding $\{\alpha_i\}_{i=1}^N$ based on a constant Δp as in Algorithm 2. The target SPDP sequence $\{p_i\}_{i=1}^N$ is obtained by interpolation $p_i = (1 - \frac{i-1}{N-1})p^{(0)} + \frac{i-1}{N-1}p^{(1)}$, where the two endpoints are $p^{(0)} = [0, 1]^T$ and $p^{(1)} = [1, 0]^T$.

D. Controllable Sound Morphing with Discrete α Series

Once a perceptually uniform discrete morph factor sequence $\{\alpha_i\}_{i=1}^N$ is obtained, we can further extend it to different sound morphing methods discussed in Section III-A.

Static morphing. To achieve controllable static morphing, we control the target SPDP point p , which represents how the desired output perceptually intermediate between $x^{(0)}$ and $x^{(1)}$. We find the corresponding α value by the binary search with the target p and further obtain a morphed result $x^{(\alpha)}$.

Cyclostationary morphing. To produce N perceptually uniform hybrid sounds between $x^{(0)}$ and $x^{(1)}$, we first obtain N uniform interpolated SPDP points $\{p_i\}_{i=1}^N$. Then we find corresponding morph factors $\{\alpha_i\}_{i=1}^N$ and further obtain N morphed results $\{x^{(\alpha_i)}\}_{i=1}^N$.

Dynamic morphing. Dynamic morphing performs sound morphing over time, one challenge is that if the morphing path fails to ensure perceptual intermediateness and audio description correspondence, the resulting sounds may exhibit

TABLE I

TIMBRAL MORPHING FOR MUSICAL INSTRUMENTS COMPARED TO THE BASELINE ON DIFFERENT INSTRUMENTS.							
Group	Method	FAD ↓	FID ↓	CDPAM _T ↓	CDPAM _{mean±std} ↓	\mathcal{L}_2^{timbre} ↓	CDPAM _E ↓
Piano ↔ Guitar	SMT	24.73	102.57	1.170	0.116 ± 0.074	1.263	0.122
	Ours	5.21	41.11	0.404	0.044 ± 0.020	0.466	0.132
Harp ↔ Kalimaba	SMT	13.46	88.89	1.495	0.150 ± 0.117	1.355	0.182
	Ours	4.67	37.92	0.768	0.076 ± 0.089	0.462	0.159
Taiko ↔ Hihat	SMT	8.51	131.57	2.339	0.234 ± 0.332	1.584	0.732
	Ours	3.32	47.59	1.314	0.131 ± 0.058	0.359	0.102
Piano ↔ Violin	SMT	21.38	90.63	1.902	0.190 ± 0.069	0.558	0.217
	Ours	3.42	20.14	0.782	0.078 ± 0.020	0.415	0.085
Piano ↔ Organ	SMT	21.36	63.26	1.291	0.129 ± 0.074	1.106	0.097
	Ours	3.29	19.73	0.233	0.023 ± 0.010	0.423	0.097

Algorithm 2 Binary search with constant Δp

Require: α_{start} : start alpha value; α_{end} : end alpha value; N : interpolate number; source audio $x^{(0)}$; target audio $x^{(1)}$;

Ensure: $p_{list} = []$, $p_{start} = [0, 1]^T$, $p_{end} = [1, 0]^T$; $\alpha_{list} = []$, $\alpha_{start} = 0$, $\alpha_{end} = 1$;

Step 1: Obtain target SPDP points with constant Δp .

Procedure ConstantSPDP(N, p_{start}, p_{end})

for i **from** 1 **to** $N - 1$ **do**

$$t \leftarrow \frac{i}{N-1}$$

$$p_i \leftarrow (1 - t) \times p_{start} + t \times p_{end}$$

$$p_{list} \leftarrow p_{list} \cup [p_i]$$

end for

Step 2: Perform binary search given target SPDP points.

Procedure BinarySearch($\alpha_{start}, \alpha_{end}, x^{(0)}, x^{(1)}, p_{list}, \epsilon_{tol}$)

$\alpha_{list} \leftarrow [\alpha_{start}]$, $\alpha_{cur} \leftarrow \alpha_{start}$;

for p_i **from** p_1 **to** p_{N-2} **do**

$$p_{target} \leftarrow p_i$$

$$\alpha_{t1} \leftarrow \alpha_{cur}, \alpha_{t2} \leftarrow \alpha_{end}$$

$$\alpha_{mid} \leftarrow \frac{\alpha_{t1} + \alpha_{t2}}{2}$$

$$p_{mid} \leftarrow SPDP(x^{\alpha_{mid}}, x^{(0)}, x^{(1)})$$

while $|p_{mid} - p_i| > \epsilon_{tol}$ **do**

if $p_{mid} > p_{target}$ **then**

$$\alpha_{t2} \leftarrow \frac{\alpha_{t1} + \alpha_{t2}}{2}$$

else

$$\alpha_{t1} \leftarrow \frac{\alpha_{t1} + \alpha_{t2}}{2}$$

end if

$$\alpha_{mid} \leftarrow \frac{\alpha_{t1} + \alpha_{t2}}{2}$$

$$p_{mid} \leftarrow SPDP(x^{\alpha_{mid}}, x^{(0)}, x^{(1)})$$

end while

$$\alpha_{list} \leftarrow \alpha_{list} \cup [\alpha_{mid}]$$

end for

return α_{list}

perceptual discontinuities or unnatural intermediate stages. SoundMorpher produces perceptually uniform sound morphing sequences, which can avoid the problem when performing dynamic morphing. We obtain N interpolated target SPDP points $\{p_i\}_{i=1}^N$ with Δp . The corresponding morph factors $\{\alpha_i\}_{i=1}^N$ are determined by binary search with the target SPDP points. Each morphed latent variable $z^{(\alpha_i)}$ contributes a segment of length $\frac{K}{N}$, where K is the length of latent variables, producing a latent variable segment $\tilde{z}^{(\alpha_i)}$ according to index i . The final morphed audio sample can be obtained by

$$x_{morph} = \text{vocoder}(\text{decoder}(\text{concat}(\tilde{z}^{(\alpha_1)}, \dots, \tilde{z}^{(\alpha_N)}))) \quad (10)$$

V. EXPERIMENT

In this section, we show three applications of SoundMorpher in real-world scenarios: *Timbral morphing for musical instruments*, *Environmental sound morphing*, and *Music morphing*.

A. Evaluation Metric

We systematically verify SoundMorpher according to the criteria mentioned in Section III-A, with a series of adapted quantitative objective metrics as below

- **Correspondence.** We design a metric that computes absolute error for the mid-point MFCCs proportion, namely $\text{MFCCs}_{\mathcal{E}}$, for descriptive correspondence. Let N be an odd integer, We define a series of perceptually uniform morphing results $\{x^{(\alpha_i)}\}_{i=1}^N$ with source and target audio $x^{(0)}$ and $x^{(1)}$, where i in the range of 1 to N . The $\text{MFCCs}_{\mathcal{E}}$ is computed by

$$\text{MFCCs}_{\mathcal{E}} = \text{abs} \left(\frac{\|m^{(\frac{N+1}{2})} - m^{(0)}\|_2}{\|m^{(\frac{N+1}{2})} - m^{(0)}\|_2 + \|m^{(\frac{N+1}{2})} - m^{(1)}\|_2} - 0.5) \right) \quad (11)$$

where $m^{(i)}$ represents the extracted MFCCs feature of the i^{th} morphed results in the series $x^{(\alpha_i)}$, $m^{(0)}$ and $m^{(1)}$ represents MFCCs feature of $x^{(0)}$ and $x^{(1)}$. This metric aims to evaluate spectrogram coherent of the midpoint result $x^{(\frac{N+1}{2})}$ between two end points $x^{(0)}$ and $x^{(1)}$, which MFCCs captures *low-level* of audio descriptive information [59], [60]. Ideally, we wish the midpoint morphed result contains half-and-half audio description elements on two end points. The larger $\text{MFCCs}_{\text{error}}$ indicates the audio description consistency is far away than the midpoint (i.e., 0.5). We extract MFCCs feature with 13 coefficients to compute $\text{MFCCs}_{\mathcal{E}}$.

We use *Fréchet audio distance* (FAD) [61] and *Fréchet inception distance* (FID) [62] between morphed audios and sourced audios to verify semantic distribution similarity between morphed samples and sourced audios. Both metrics capture *high-level* of semantic audio descriptive information by extracting audio features from pretrained audio classification models. Given two sets of audio X_{mvp} and X_{src} , where X_{mvp} contains consecutive morphed samples as $X_{mvp} = \{x^{(\alpha_i)}\}_{i=1}^N$, and X_{src} contains sourced audio samples¹. We calculate FAD and FID

¹In environmental sound morphing task, we set all sourced sounds in that class as X_{src} .

values based on audio features extracted by pretrained audio classification models between X_{src} and X_{mrp} ².

- **Intermediateness.** CDPAM [63] is a metric designed to evaluate the perceptual similarity between audio signals, which is commonly used in domains such as speech [63], music [64] and environmental sound [65]. We use total CDPAM by $CDPAM_T = \sum_{i=1}^{N-1} CDPAM(x^{(\alpha_i)}, x^{(\alpha_{i+1})})$ for morph sequence to reflect direct perceptual intermediateness. A smaller $CDPAM_T$ indicates the morph sequence exhibits higher perceptual intermediate similarity between consecutive sounds, suggesting intermediate consistency.
- **Smoothness.** We calculate the mean and standard deviation of CDPAM along with the morphing path to validate smoothness, as $CDPAM_{mean \pm std} = CDPAM_{mean} \pm CDPAM_{std}$, where $CDPAM_{mean} = \frac{1}{N-1} \sum_{i=1}^{N-1} CDPAM(x^{(\alpha_i)}, x^{(\alpha_{i+1})})$, and $CDPAM_{std} = \sqrt{\frac{1}{N-1} \sum_{i=1}^{N-1} (CDPAM(x^{(\alpha_i)}, x^{(\alpha_{i+1})}) - CDPAM_{mean})^2}$. In timbre study, we define *timbral distance* as \mathcal{L}_2^{timbre} by $\mathcal{L}_2^{timbre} = \frac{1}{N-1} \sum_{i=1}^{N-1} \|q^{(\alpha_{i+1})} - q^{(\alpha_i)}\|_2$, where $q^{(\alpha_i)}$ represents the corresponding timber point of $x^{(\alpha_i)}$ in timbre space [66].
- **Reconstruction of perceptual correspondence.** Lastly, we denote $CDPAM_E$ that calculate CDPAM between $\{x^{(0)}, x^{(1)}\}$ and $\{\hat{x}^{(0)}, \hat{x}^{(1)}\}$, where \hat{x} represents resynthesized end points when $\alpha = 0$ and $\alpha = 1$.

B. Timbral Morphing for Musical Instruments

Sound morphing can allow timbral morphing between the sound of two known musical instruments, creating sounds from unknown parts of the timbre space [67], [68]. Timbral morphing for musical instruments involves transitioning between timbres of two different musical instruments to create a new sound. This new sound could possess characteristics of both original timbres as well as new timbral qualities between them, which usually applied to creative arts. In this experiment, we perform timbral morphing for isolated musical instruments given two recordings of the same musical composition played by different music instruments.

Dataset. To ensure high quality of paired compositions on timbral study, we selected 22 paired musical instrument composition samples from demonstration pages of musical timbre transform projects, MusicMagus [30] and Timbrer [69]. The paired samples have durations varies from 5s to 10s, with 16.0kHz and 44.01kHz, which involve 5 groups of instrument pairs: 2 paired samples of piano-violin; 10 paired samples of piano-guitar; 1 paired sample of taiko-hihat; 1 paired sample of piano-organ, and 8 paired samples of harp-kalimaba.

Baseline. We compare with Sound Morphing Toolbox (SMT) [11], a set of Matlab functions targeting on musical instrument morphing. SMT implements a sound morphing algorithm for isolated musical instrument sounds. Since SMT performs sound morphing based on the linear assumption [16], we uniformly interpolate 11 morph factors in $[0, 1]$.

Results and analysis. The comparison of our method and the baseline on timbral morphing is in Table I. Overall, SoundMorpher demonstrates superior morphing quality compared to STM across various metrics, including audio quality, intermediateness, smoothness, and resynthesis quality ³, when applied to different types of musical instrument timbre morphing. Notably, STM fails in Taiko-Hihat timbral morphing due to significant high reconstruction perceptual error. In contrast, SoundMorpher maintains robustness across different types of musical instruments, making it a more flexible and efficient solution for timbral morphing applications on different types of musical instruments. It is not surprising that SMT has poor performance in this experiment, since the traditional signal processing sound morphing methods are limited to complex or inharmonic sounds [12]. Figure. 2 provides a visualization of normalized timbre space, illustrating morphing trajectories generated by SMT and SoundMorpher. The timbre space is defined by three important timbral features: Log-Attack Time, Spectral Centroid, and Spectral Flux [66], [67]. The SMT trajectory shows distinct steps, indicating that the transitions between each intermediate sound are relatively abrupt. The spacing between the blue points suggests that each step represents a significant change in timbre, which may result in a less smooth perceptual transition between two musical instruments. In contrast, the trajectory produced by SoundMorpher demonstrates a smoother curve. The points are more closely spaced, indicating more gradual changes between each intermediate timbre. This suggests that SoundMorpher achieves a more continuous and natural-sounding morphing process, with each step being a smaller, more refined adjustment compared to SMT. Fig. 3 provides spectrogram visualization of how SoundMorpher performs timbre morphing.

C. Environmental Sound Morphing

Environmental sounds are used in video game production to provide a sense of presence within a scene. For example, in video, AR and VR games, sound morphing could enhance user immersion by adapting audio cues to specific visual and interactive contexts. This means that it could be useful to morph between sonic locations, e.g., a city and a park, or between sound effects, e.g., different animal sounds to represent fantasy creatures. In this experiment, we perform cyclostationary morphing with $N = 5$ by SoundMorpher across various types of environmental sounds.

Dataset. In this experiment, we firstly use ESC50 [70] to study the robustness of SoundMorpher across different categories of environmental sounds. Then we make a direct comparison with a concurrent method, MorphFader [13], based on environmental sounds provided in ⁴. ESC50 [70] which consists of 5-second recordings organized into 50 semantic classes which loosely arranged into 5 major categories. We randomly select 4 major categories of scenarios to verify our method, including (1) Dog-Cat (animals voices), (2) Laughing-Crying baby (human sounds), (3) Church bells-Clock alarm

³Since we perform timbral morphing within the same music composition, MFCCs_E may not a suitable metric under the same musical content. In contrast, we focus on evaluating smoothness and intermediateness.

⁴<https://pkmath2.github.io/audio-morphing-with-text/webpage/index.html>

²The FAD and FID metrics are obtained based on https://github.com/haoheliu/audioldm_eval

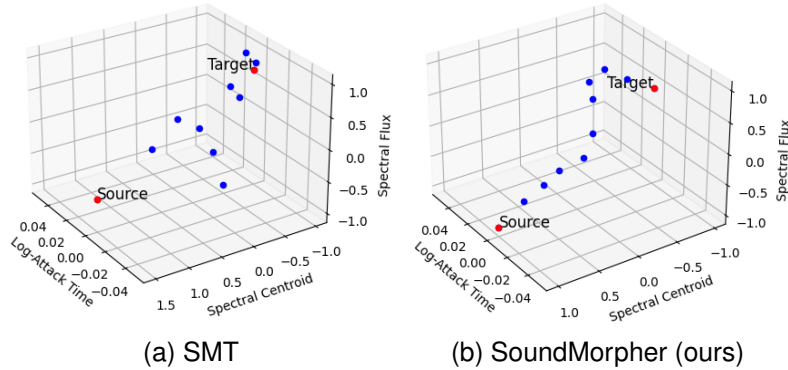


Fig. 2. Timbre space visualization of morph trajectories for piano-organ timbre morphing. Compared to SMT, SoundMorpher produces a smoother and continuous morph in the timbre space.

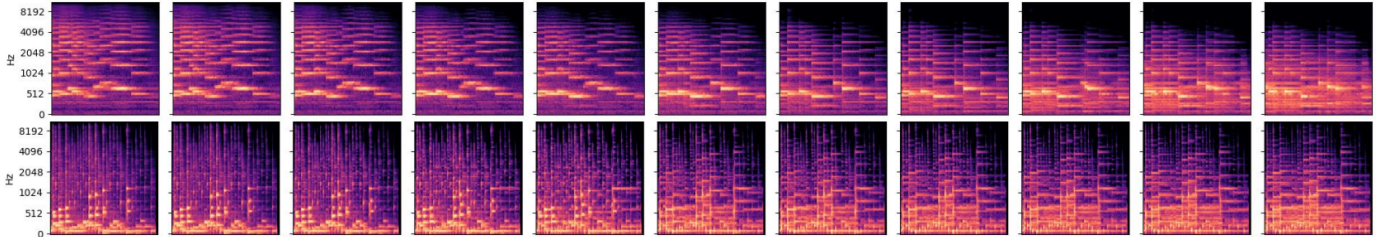


Fig. 3. Visualization of timbre morphing for musical instruments with $N = 11$ by SoundMorpher compared to SMT.

TABLE II
ENVIRONMENTAL SOUND MORPHING WITH DIFFERENT TYPES OF ENVIRONMENTAL SOUNDS.

Category	FAD _{category}	MFCCs _{\mathcal{E}} ↓	FAD↓	FID↓	CDPAM _T ↓	CDPAM _{mean±std} ↓	CDPAM _E ↓
Dog ↔ Cat	26.08	0.081	17.77	73.92	1.293	0.323 ± 0.160	0.236
Laughing ↔ Crying baby	10.39	0.044	9.35	65.98	0.855	0.214 ± 0.077	0.289
Church bells ↔ Clock alarm	68.29	0.058	22.89	75.77	2.205	0.551 ± 0.299	0.312
Door knock ↔ Clapping	21.36	0.083	10.85	76.35	1.594	0.428 ± 0.220	0.321

TABLE III
COMPARISON WITH MORPHFADER

Method	CDPAM _T	CDPAM _{mean±std}	MFCCs _{\mathcal{E}}
MorphFader	0.972	0.243 ± 0.139	0.065
SoundMorpher	0.935	0.226 ± 0.162	0.065

(urban noise-interior sound), (4) Door knock-clapping (interior sounds-human sounds). Each category of scenarios contains 25 randomly selected audio pairs, thereby, 100 randomly paired samples in total. To have a fair comparison, we also perform environmental sound morphing based on samples provided by MorphFader, which is sourced from AudioPairBank [71].

Baseline. Due to lack of open-sourced direct comparison, we compare SoundMorpher with MorphFader [13] based on the criteria outlined in Section III-A. Although MorphFader didn’t release their codes, our evaluation system still can make a fair comparison based on their demonstrated examples.

Results and analysis. We first apply SoundMorpher on ESC50 dataset to study how SoundMorpher performs on different categories of environmental sounds. Table II presents the results of applying SoundMorpher to various categories of environmental sounds. To quantify the semantic gap between sound scene classes, we calculate FAD between them as FAD_{category}. The results demonstrate SoundMorpher is capable of effectively morphing a wide range of environmental sounds. However, environmental sounds with a large semantic

gap between categories can negatively impact the morphing quality. Additionally, we observe that the quantitative metrics for morphing quality and reconstruction perceptual errors in this experiment are higher than those for the timbre morphing task. One reason is the inherent complexity of environmental sounds, which often involve intricate physical events with significant temporal structure differences and background noises, making them more challenging to morph compared to musical data. Fig. 5 provides spectrogram visualizations on environmental sound morphing.

We then make a direct comparison with the concurrent method, MorphFader [13], based on their demonstrated morphed samples in Table III⁵. SoundMorpher produces a smoother and intermediate morph than MorphFader with improvement on CDPAM_T and CDPAM_{mean}. Fig. 4 provides a direct visual comparison of a morph sequence produced by MorphFader and our method. The yellow rectangles in Fig. 4 highlight frequency band intensity cross morphing results. The intensity of the frequency bands within the yellow rectangle changes more abruptly for MorphFader, in contrast, SoundMorpher are more stable and consistent across time. This suggests that SoundMorpher maintains better spectral consistency during the morphing process, with smoother transitions

⁵Due to the demonstration page doesn’t provide original audio samples, we cannot compute FAD, FID and CDPAM_E for this comparison.

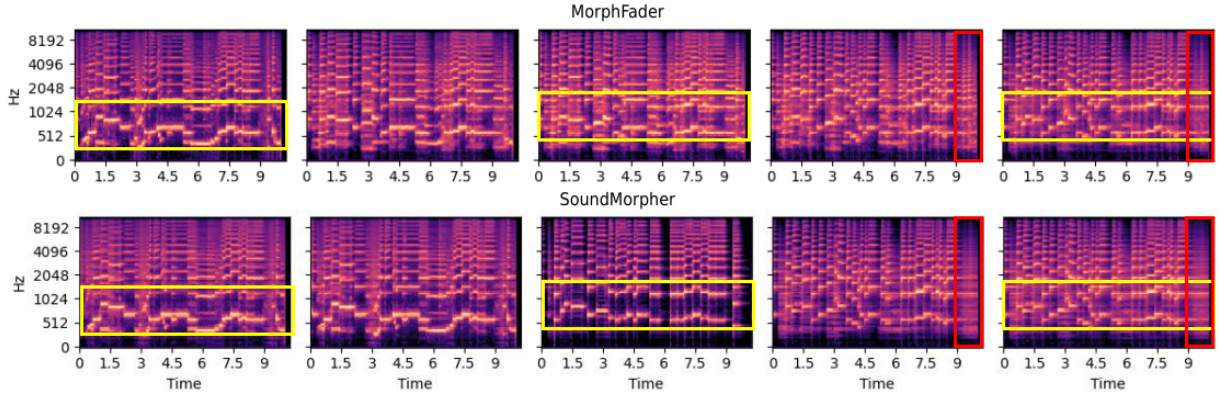


Fig. 4. Visualization of spectrogram for morphed results compared with MorphFader. SoundMorpher appears to provide a more seamless and stable morphing process, in which transitions are smoother and the spectral content is more consistent across the morphing stages.

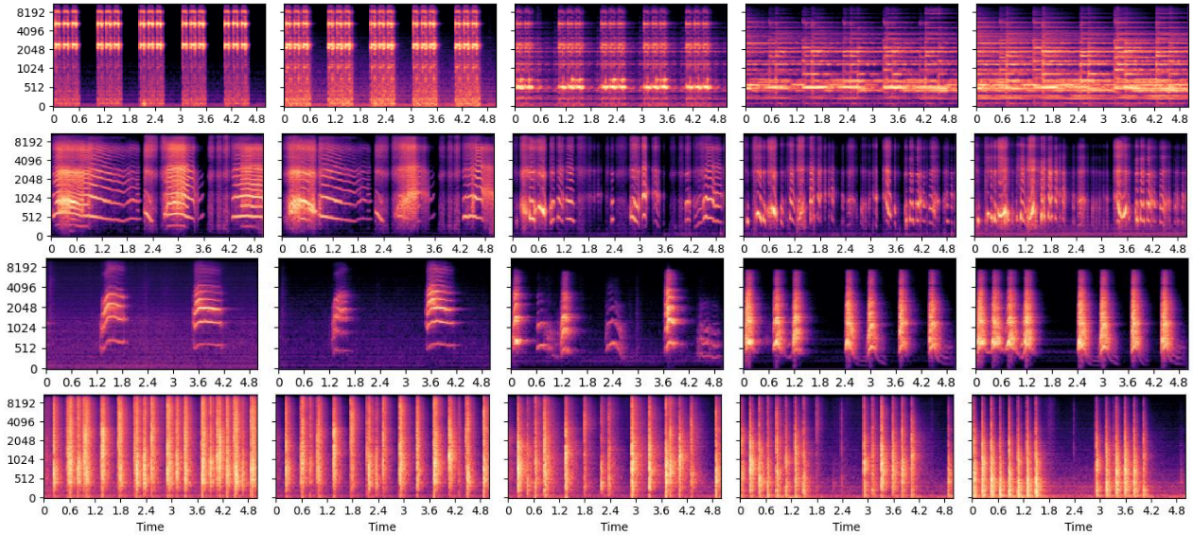


Fig. 5. Visualization of environmental sound morphing with $N = 5$, from top to bottom: (1) church bells \leftrightarrow clock alarm (2) crying baby \leftrightarrow laughing (3) cat \leftrightarrow dog (4) clapping \leftrightarrow wood door knocking

between different timbral characteristics. As red rectangles indicate, MorphFader introduces more abrupt changes at the end of the morphing sequence. There is a noticeable shift in the pattern, indicating less smoothness on transition. In contrast, SoundMorpher shows a more gradual and consistent transition within the red rectangles. The spectral patterns remain more stable and exhibit smoother transitions towards the end of the morphing sequence. Overall, SoundMorpher appears to provide a more seamless and stable morphing process. The transitions are smoother, and the spectral content is more consistent across the morphing stages.

D. Music Morphing

Film or game post-production often requires blending or fading between music tracks to seamlessly transition background music in between scenes. Music morphing transitions between two music compositions without cross fading, that is, each moment of the morphed music would be a single composition with elements that are perceptually in between both source and target music, rather than simply blending the two together. Different from timbral morphing, music morphing could ideally be accomplished with compositions

from different genres and mixed musical instruments. In this experiment, we use SoundMorpher to perform dynamic morphing on music with $N = 15$.

Dataset. Motivated by [30], we randomly selected 50 sample pairs from 20 high-quality musical samples available on AudioLDM2 [42] demonstration page. These 10-second music compositions that span different genres and feature both single or mixed musical instrument arrangements.

Baseline. Due to lack of direct comparison on dynamic music morphing, we set the baseline as SoundMorpher without SPDP binary search, which achieves sound morphing by smoothly interpolate condition embeddings and latent states. We uniformly sample 15 morph factors in $\alpha \in [0, 1]$ as the baseline for comparison.

Results and analysis. Even though this experiment contains morph complex music compositions with different music genres and music instruments, Table IV shows our method superiors on perceptual smoothly transiting source music to the target music and ensures correspondence, intermediateness and smoothness compared to the baseline, which further illustrates the advantage of the proposed algorithm of SPDP with binary search. Fig. 6 visually demonstrates the effectiveness of the

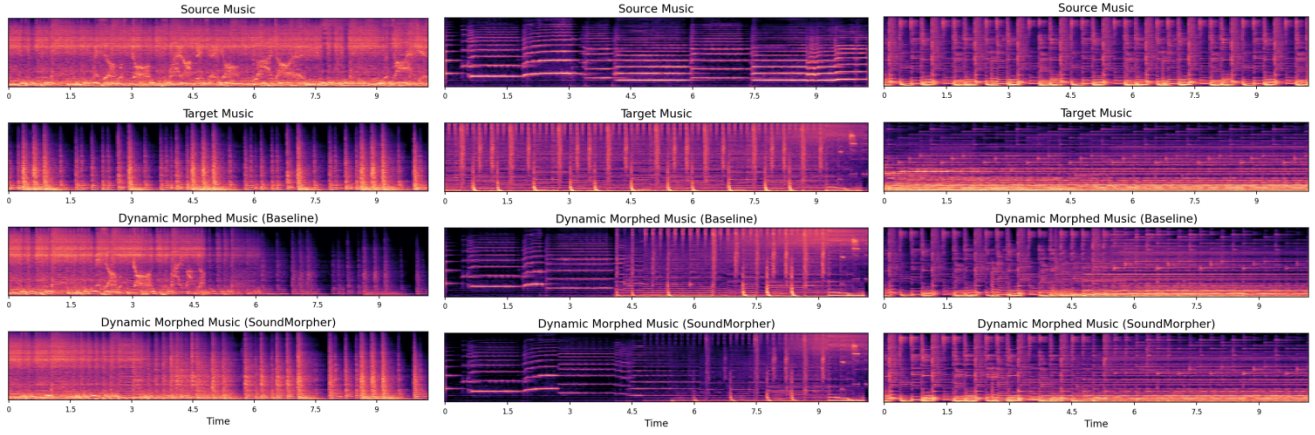


Fig. 6. Visualization of dynamic morphed music for SoundMorpher and baseline with $N = 15$, source music and target music.

TABLE IV
MUSIC MORPHING EXPERIMENTAL RESULTS, BASELINE COMPARISON & ABLATION STUDY FOR SOUND PERCEPTUAL FEATURES

Method	MFCCs $_{\epsilon}$ ↓	FAD ↓	FID ↓	CDPAM $_T$ ↓	CDPAM $_{mean \pm std}$ ↓	CDPAM $_E$ ↓
Baseline (Mel-Spec.)	0.099	10.82	58.20	0.938	0.067 ± 0.065	0.158
SoundMorpher (Mel-Spec.)	0.047	9.85	56.25	0.847	0.068 ± 0.045	0.178
Reduced Mel-Spec. (n=2)	0.187	10.31	58.57	0.793	0.056 ± 0.075	0.182
Reduced Mel-Spec. (n=3)	0.151	10.76	59.39	0.779	0.055 ± 0.079	0.151
MFCCs	0.053	10.11	57.38	0.987	0.071 ± 0.050	0.156
Spectral Contrast	0.066	10.54	58.44	0.863	0.061 ± 0.071	0.155

* where n represents the number of components of PCA for reducing dimension of Mel-spectrogram

proposed dynamic morphing method in transitioning smoothly from source to target music while ensuring perceptual consistency and intermediate transformations. Compared to the baseline results, which exhibit noticeable abrupt changes and spectral discontinuities, SoundMorpher produces gradual and smooth spectral transitions over time. This highlights that simply linearly interpolating semantic features, as done in the baseline method, fails to achieve truly smooth and perceptually consistent sound morphing.

E. Discussion And Ablation Study

Ablation study on sound perceptual features. We verified the perceptual feature in SPDP in music morphing task. We select alternative music information retrieval features (MIR) including MFCCs with 13 coefficients [60], and Spectral contrast [72]. We use principal component analysis (PCA) to reduce the dimensionality of Mel-spectrogram to further capture variation of spectral content over time, which is referred to as reduced Mel-Spec. [55], [72], [73]. Table IV shows performance comparisons of SoundMorpher with different features, SoundMorpher with Mel-spectrogram achieves better morphing quality in terms of correspondence and smoothness variation with smaller FAD, FID and CDPAM $_{std}$. While Mel-spectrogram yields higher CDPAM $_{mean}$, CDPAM $_T$ and MFCCs $_{\epsilon}$ compared to reduced Mel-Spec. and MFCCs, the differences in metric values are not significant. However, the overall morph quality with Mel-spectrogram is consistently better than other features. This suggests Mel-spectrogram, as a pseudo-3D representation, provide more perceptual and semantic information, which contributes to improve morph quality compared to higher-level features.

Uninformative v.s. informative initial text prompt. Complex audio usually cannot easily yield precise information to users. For example, it is a challenge for non-professional users to describe the genre of a music. We conduct an ablation study for initial text prompt on music morphing to verify effectiveness of text-guided conditional embedding optimization. We use a general initial text prompt, ‘a sound clip of music composition.’, as an uninformative initial prompt. And we use the given text prompts in AudioLDM2⁶ as informative initial prompts. As in Table V, informative initial text prompts may help with resynthesis quality and further improves morph correspondence. Despite the improved resynthesis quality with informative initial text prompts, the results show a decline in morphing intermediateness and smoothness. One possible reason is the better resynthesis quality makes the resynthesis endpoints more distinct (i.e., larger semantic gap), which could lead to slight decline in intermediateness and smoothness. However, the performance difference on initial text prompts is not significant which illustrates effectiveness of conditional embedding optimization.

Inference steps. In our experiment, we follow the configuration of [30] and set DDIM steps to 100. To verify whether DDIM steps affect SoundMorpher performances, we compare with 20 DDIM steps in Table V. Larger inference step seems to help for reconstruction quality and slightly improves morph quality, however, performance differences between inference steps are not significant. This indicates SoundMorpher is robust for inference steps; therefore, we suggest selecting a suitable DDIM step to trade-off overall binary search algorithm time-consuming and morph quality.

Ablation study on LoRA rank. In this experiment, we conduct an ablation study on model adaptation with LoRA

⁶<https://audioldm.github.io/audioldm2/>

TABLE V
EXPERIMENT AND ABLATION STUDY RESULTS ON MUSIC MORPHING.

Init. text	T = 20	T = 100	MFCCs $_{\mathcal{E}}$ ↓	FAD ↓	FID ↓	CDPAM $_T$ ↓	CDPAM $_{mean \pm std}$ ↓	CDPAM $_E$ ↓
Informative	✓		0.047	10.21	56.62	1.213	0.086 ± 0.069	0.166
Informative		✓	0.044	10.21	56.13	1.077	0.084 ± 0.066	0.155
Uninformative	✓		0.057	10.37	55.89	1.036	0.074 ± 0.049	0.211
Uninformative		✓	0.047	9.85	56.25	0.847	0.068 ± 0.045	0.178

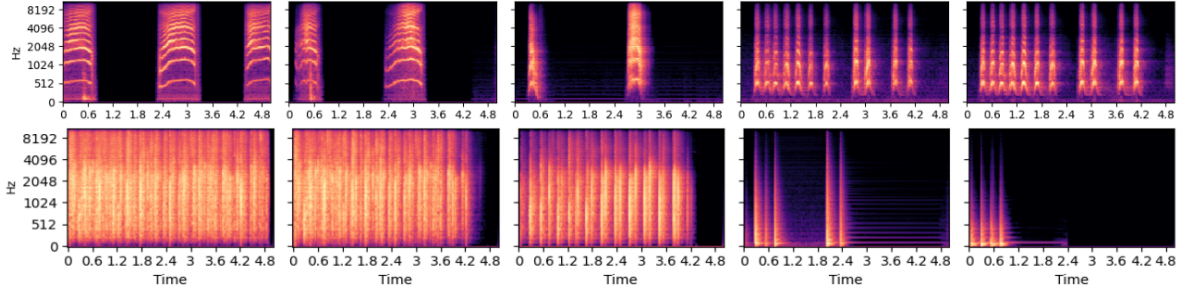


Fig. 7. Failure cases for SoundMorpher with $N = 5$. The source (left first) and target (right first) sounds that have significant semantic difference in contents, this leads SoundMorpher to produce abrupt transitions.

TABLE VI
ABLATION STUDY ON MODEL ADAPTATION WITH DIFFERENT LORA RANK r ON MUSIC MORPHING. RANK WITH — REPRESENTS RESULTS WITHOUT LORA MODEL ADAPTATION.

Rank	MFCCs $_{\mathcal{E}}$ ↓	FAD ↓	FD ↓	CDPAM $_T$ ↓	CDPAM $_{mean \pm std}$ ↓	CDPAM $_E$ ↓
—	0.073	10.38	56.02	1.052	0.085 ± 0.054	0.198
4	0.047	9.85	56.25	0.847	0.068 ± 0.045	0.178
8	0.059	10.01	56.35	1.035	0.073 ± 0.051	0.180
16	0.059	9.95	56.14	1.058	0.075 ± 0.052	0.169
32	0.130	10.77	59.06	0.818	0.058 ± 0.082	0.158

on the task of music morphing. We test SoundMorpher with different LoRA ranks as well as SoundMorpher without model adaptation. Following [52], we train LoRA parameters for 150 steps with 1e-3 learning rate. We also set unconditional bias correction with $r_0 = 2$ for 15 steps with 1e-3 learning rate. Table VI shows the results of SoundMorpher with different rank size on model adaptation settings. According to Table VI, SoundMorpher without model adaptation has obvious performance drop on morphing correspondence compares results with LoRA model adaptation. Even though a higher LoRA rank has a slight improvement on perceptual reconstruction quality, however, SoundMorpher with $r = 32$ indicates poor correspondence with large MFCCs $_{\mathcal{E}}$ and large smoothness variance CDPAM $_{std}$. This result indicates that SoundMorpher with higher LoRA rank not lead to a better morphing quality. When $r = 4$, SoundMorpher achieves the best performance on smoothness, and correspondence compared to $r = 8$, $r = 16$ and $r = 32$. Therefore, we suggest LoRA rank for model adaptation in SoundMorpher shouldn't be too large.

Limitations. Although SoundMorpher is the first open-world sound morphing method, offering high-quality morphed results and broad applicability, we have identified the following limitations: The current implementation of SoundMorpher based on AudioLDM2 with 16.0kHz sampling rate, which may limit output audio quality. The conditional embeddings optimization only applies to sounds that can be produced by AudioLDM2. Sound examples that close to white noise, such as pure wind blowing used in MorphGAN [12] are not easily generated by AudioLDM2, which makes the conditional embedding optimization produce low-quality resynthesis sounds.

Although SoundMorpher produces high-quality sound morphing results, abrupt transitions can occur when the source and target sounds have significant temporal structure differences. A clear example of this is attempting to morph continuous environmental sounds with sounds that contain more silence, as in Fig. 7. Environmental sounds often consist of discrete and temporally separated events, such as a dog barking or a cat meowing, which have distinct and abrupt characteristics. These are inherently different from the more continuous and harmonically structured nature of music, where elements blend more fluidly over time. As a result, creating smooth transitions between such disjointed environmental sounds can be more challenging, leading to the perception of more abrupt or less natural transitions in the morphing process.

VI. CONCLUSION

We propose SoundMorpher, a open-world sound morphing method base on a pretrained diffusion model that produces perceptually uniform morph trajectories. Unlike existing methods, we refined the sound morphing problem and explored a more complex connection between morph factor and perception of morphed results which offers better flexibility and higher morphing quality, making it adaptable to various morphing methods and real-world scenarios. We validate SoundMorpher with a series of adapted objective quantitative metrics following three format sound morphing criterions proposed by [16]. These quantitative metrics may help to formalize future studies for direct comparison on sound morphing evaluation. Furthermore, we demonstrated that SoundMorpher can be applied to wide range of real-world applications in our experiments and

conducted in-depth discussions. SoundMorpher also has the potential to achieve voice morphing, as its foundational model AudioLDM2 supports speech generation; however, we leave this exploration for future work.

REFERENCES

- [1] M. Caetano and X. Rodet, "Sound morphing by feature interpolation," in *2011 IEEE International Conference on Acoustics, Speech and Signal Processing (ICASSP)*. IEEE, 2011, pp. 161–164.
- [2] J. Hyrkas, "Network modulation synthesis: New algorithms for generating musical audio using autoencoder networks," *arXiv preprint arXiv:2109.01948*, 2021.
- [3] I. P. Qamar, K. Stawarz, S. Robinson, A. Goguy, C. Coutrix, and A. Roudaut, "Morphino: a nature-inspired tool for the design of shape-changing interfaces," in *Proceedings of the 2020 ACM Designing Interactive Systems Conference*, 2020, pp. 1943–1958.
- [4] S. Siddiq, "Real-time morphing of impact sounds," in *Audio Engineering Society Convention 139*. Audio Engineering Society, 2015.
- [5] E. Tellman, L. Haken, and B. Holloway, "Timbre morphing of sounds with unequal numbers of features," *Journal of the Audio Engineering Society*, vol. 43, no. 9, pp. 678–689, 1995.
- [6] N. Osaka, "Timbre interpolation of sounds using a sinusoidal model," *Proc. of ICMC*, 1995, 1995.
- [7] D. Williams, P. Randall-Page, and E. R. Miranda, "Timbre morphing: near real-time hybrid synthesis in a musical installation." in *NIME*, 2014, pp. 435–438.
- [8] T. Brookes and D. Williams, "Perceptually-motivated audio morphing: Warmth," in *Audio Engineering Society Convention 128*. Audio Engineering Society, 2010.
- [9] M. F. Caetano and X. Rodet, "Automatic timbral morphing of musical instrument sounds by high-level descriptors," in *International Computer Music Conference*, 2010, pp. 11–21.
- [10] G. Roma, O. Green, and P. A. Tremblay, "Audio morphing using matrix decomposition and optimal transport," in *Proceedings of DAFX*, 2020.
- [11] M. Caetano, "Morphing musical instrument sounds with the sinusoidal model in the sound morphing toolbox," in *International Symposium on Computer Music Multidisciplinary Research*. Springer, 2019, pp. 481–503.
- [12] C. Gupta, P. Kamath, Y. Wei, Z. Li, S. Nanayakkara, and L. Wyse, "Towards controllable audio texture morphing," in *ICASSP 2023-2023 IEEE International Conference on Acoustics, Speech and Signal Processing (ICASSP)*. IEEE, 2023, pp. 1–5.
- [13] P. Kamath, C. Gupta, and S. Nanayakkara, "Morphfader: Enabling fine-grained controllable morphing with text-to-audio models," *arXiv preprint arXiv:2408.07260*, 2024.
- [14] Y. Zou, J. Liu, and W. Jiang, "Non-parallel and many-to-one musical timbre morphing using ddspp-autoencoder and spectral feature interpolation," in *2021 International Conference on Culture-oriented Science & Technology (ICCST)*, 2021, pp. 144–148.
- [15] J. W. Kim, R. Bittner, A. Kumar, and J. P. Bello, "Neural music synthesis for flexible timbre control," in *ICASSP 2019 - 2019 IEEE International Conference on Acoustics, Speech and Signal Processing (ICASSP)*, 2019, pp. 176–180.
- [16] M. Caetano and N. Osaka, "A formal evaluation framework for sound morphing," in *ICMC*, 2012.
- [17] M. Caetano and X. Rodet, "Musical instrument sound morphing guided by perceptually motivated features," *IEEE Transactions on Audio, Speech, and Language Processing*, vol. 21, no. 8, pp. 1666–1675, 2013.
- [18] A. Primavera, F. Piazza, and J. D. Reiss, "Audio morphing for percussive hybrid sound generation," in *Audio Engineering Society Conference: 45th International Conference: Applications of Time-Frequency Processing in Audio*. Audio Engineering Society, 2012.
- [19] M. Caetano, "Morphing isolated quasi-harmonic acoustic musical instrument sounds guided by perceptually motivated features," Ph.D. dissertation, Paris 6, 2011.
- [20] S. Kazazis, P. Depalle, and S. McAdams, "Sound morphing by audio descriptors and parameter interpolation," in *Proceedings of the 19th International Conference on Digital Audio Effects (DAFx-16)*. Brno, Czech Republic, 2016.
- [21] J. Engel, L. Hantrakul, C. Gu, and A. Roberts, "Ddsp: Differentiable digital signal processing," *arXiv preprint arXiv:2001.04643*, 2020.
- [22] J. Engel, C. Resnick, A. Roberts, S. Dieleman, M. Norouzi, D. Eck, and K. Simonyan, "Neural audio synthesis of musical notes with wavenet autoencoders," in *International Conference on Machine Learning*. PMLR, 2017, pp. 1068–1077.
- [23] Y.-J. Luo, K. Agres, and D. Herremans, "Learning disentangled representations of timbre and pitch for musical instrument sounds using gaussian mixture variational autoencoders," *arXiv preprint arXiv:1906.08152*, 2019.
- [24] H. H. Tan, Y.-J. Luo, and D. Herremans, "Generative modelling for controllable audio synthesis of expressive piano performance," *arXiv preprint arXiv:2006.09833*, 2020.
- [25] H. Liu, Z. Chen, Y. Yuan, X. Mei, X. Liu, D. Mandic, W. Wang, and M. D. Plumbley, "Audioldm: Text-to-audio generation with latent diffusion models," *arXiv preprint arXiv:2301.12503*, 2023.
- [26] G. Le Vaillant and T. Dutoit, "Interpolation of synthesizer presets using timbre-regularized auto-encoders," *Authorea Preprints*, 2023.
- [27] T. Dutoit *et al.*, "Synthesizer preset interpolation using transformer auto-encoders," *ICASSP 2023 Proceedings*, 2023.
- [28] G. Le Vaillant and T. Dutoit, "Latent space interpolation of synthesizer parameters using timbre-regularized auto-encoders," *IEEE/ACM Transactions on Audio, Speech, and Language Processing*, 2024.
- [29] H. Manor and T. Michaeli, "Zero-shot unsupervised and text-based audio editing using ddpm inversion," *arXiv preprint arXiv:2402.10009*, 2024.
- [30] Y. Zhang, Y. Ikemiya, G. Xia, N. Murata, M. Martínez, W.-H. Liao, Y. Mitsufuji, and S. Dixon, "Musicmagus: Zero-shot text-to-music editing via diffusion models," *arXiv preprint arXiv:2402.06178*, 2024.
- [31] G. L. Lan, B. Shi, Z. Ni, S. Srinivasan, A. Kumar, B. Ellis, D. Kant, V. Nagaraja, E. Chang, W.-N. Hsu *et al.*, "High fidelity text-guided music generation and editing via single-stage flow matching," *arXiv preprint arXiv:2407.03648*, 2024.
- [32] L. Comanducci, F. Antonacci, A. Sarti *et al.*, "Timbre transfer using image-to-image denoising diffusion implicit models," in *Proceedings of the 24th International Society for Music Information Retrieval Conference, Milan, Italy, November 5-9, 2023 (ISBN: 978-1-7327299-3-3)*, 2024, pp. 257–263.
- [33] D. K. Jain, A. Kumar, L. Cai, S. Singhal, and V. Kumar, "Att: Attention-based timbre transfer," in *2020 International Joint Conference on Neural Networks (IJCNN)*. IEEE, 2020, pp. 1–6.
- [34] S. Li, Y. Zhang, F. Tang, C. Ma, W. Dong, and C. Xu, "Music style transfer with time-varying inversion of diffusion models," in *Proceedings of the AAAI Conference on Artificial Intelligence*, vol. 38, no. 1, 2024, pp. 547–555.
- [35] J. Li, W. Tu, and L. Xiao, "Freevc: Towards high-quality text-free one-shot voice conversion," in *ICASSP 2023-2023 IEEE International Conference on Acoustics, Speech and Signal Processing (ICASSP)*. IEEE, 2023, pp. 1–5.
- [36] J. Yao, Y. Yang, Y. Lei, Z. Ning, Y. Hu, Y. Pan, J. Yin, H. Zhou, H. Lu, and L. Xie, "Promptvc: Flexible stylistic voice conversion in latent space driven by natural language prompts," in *ICASSP 2024-2024 IEEE International Conference on Acoustics, Speech and Signal Processing (ICASSP)*. IEEE, 2024, pp. 10 571–10 575.
- [37] X. Niu, J. Zhang, and C. P. Martin, "Hybridvc: Efficient voice style conversion with text and audio prompts," in *Interspeech 2024*, 2024, pp. 4368–4372.
- [38] Z. Sheng, Y. Ai, L.-J. Liu, J. Pan, and Z.-H. Ling, "Voice attribute editing with text prompt," *arXiv preprint arXiv:2404.08857*, 2024.
- [39] W. A. Sethares and J. A. Bucklew, "Kernel techniques for generalized audio crossfades," *Cogent Mathematics*, vol. 2, no. 1, p. 1102116, 2015.
- [40] M. Slaney, M. Covell, and B. Lassiter, "Automatic audio morphing," in *1996 IEEE International Conference on Acoustics, Speech, and Signal Processing Conference Proceedings*, vol. 2. IEEE, 1996, pp. 1001–1004.
- [41] R. Rombach, A. Blattmann, D. Lorenz, P. Esser, and B. Ommer, "High-resolution image synthesis with latent diffusion models," in *Proceedings of the IEEE/CVF conference on computer vision and pattern recognition*, 2022, pp. 10 684–10 695.
- [42] H. Liu, Y. Yuan, X. Liu, X. Mei, Q. Kong, Q. Tian, Y. Wang, W. Wang, Y. Wang, and M. D. Plumbley, "Audioldm 2: Learning holistic audio generation with self-supervised pretraining," *IEEE/ACM Transactions on Audio, Speech, and Language Processing*, 2024.
- [43] D. P. Kingma and M. Welling, "Auto-encoding variational bayes," *arXiv preprint arXiv:1312.6114*, 2013.
- [44] J. Kong, J. Kim, and J. Bae, "Hifi-gan: Generative adversarial networks for efficient and high fidelity speech synthesis," *Advances in neural information processing systems*, vol. 33, pp. 17 022–17 033, 2020.
- [45] P.-Y. Huang, H. Xu, J. Li, A. Baevski, M. Auli, W. Galuba, F. Metze, and C. Feichtenhofer, "Masked autoencoders that listen," *Advances in Neural Information Processing Systems*, vol. 35, pp. 28 708–28 720, 2022.
- [46] X. Tan, T. Qin, J. Bian, T.-Y. Liu, and Y. Bengio, "Regeneration learning: A learning paradigm for data generation," in *Proceedings of the AAAI*

- Conference on Artificial Intelligence*, vol. 38, no. 20, 2024, pp. 22 614–22 622.
- [47] A. Radford, J. Wu, R. Child, D. Luan, D. Amodei, I. Sutskever *et al.*, “Language models are unsupervised multitask learners,” *OpenAI blog*, vol. 1, no. 8, p. 9, 2019.
- [48] H. W. Chung, L. Hou, S. Longpre, B. Zoph, Y. Tay, W. Fedus, Y. Li, X. Wang, M. Dehghani, S. Brahma *et al.*, “Scaling instruction-finetuned language models,” *Journal of Machine Learning Research*, vol. 25, no. 70, pp. 1–53, 2024.
- [49] J. Ho, A. Jain, and P. Abbeel, “Denoising diffusion probabilistic models,” *Advances in neural information processing systems*, vol. 33, pp. 6840–6851, 2020.
- [50] J. Song, C. Meng, and S. Ermon, “Denoising diffusion implicit models,” *arXiv preprint arXiv:2010.02502*, 2020.
- [51] P. Dhariwal and A. Nichol, “Diffusion models beat gans on image synthesis,” *Advances in neural information processing systems*, vol. 34, pp. 8780–8794, 2021.
- [52] Z. Yang, Z. Yu, Z. Xu, J. Singh, J. Zhang, D. Campbell, P. Tu, and R. Hartley, “Impus: Image morphing with perceptually-uniform sampling using diffusion models,” *arXiv preprint arXiv:2311.06792*, 2023.
- [53] E. J. Hu, Y. Shen, P. Wallis, Z. Allen-Zhu, Y. Li, S. Wang, L. Wang, and W. Chen, “Lora: Low-rank adaptation of large language models,” *arXiv preprint arXiv:2106.09685*, 2021.
- [54] G. Tzanetakis and P. Cook, “Musical genre classification of audio signals,” *IEEE Transactions on speech and audio processing*, vol. 10, no. 5, pp. 293–302, 2002.
- [55] S. S. Stevens, J. Volkman, and E. B. Newman, “A scale for the measurement of the psychological magnitude pitch,” *The journal of the acoustical society of america*, vol. 8, no. 3, pp. 185–190, 1937.
- [56] B. L. Sturm, “An introduction to audio content analysis: applications in signal processing and music informatics by alexander lerch,” *Computer Music Journal*, vol. 37, no. 4, pp. 90–91, 2013.
- [57] M. Müller, *Fundamentals of music processing: Audio, analysis, algorithms, applications*. Springer, 2015, vol. 5.
- [58] S. S. Stevens, “The direct estimation of sensory magnitudes: Loudness,” *The American journal of psychology*, vol. 69, no. 1, pp. 1–25, 1956.
- [59] S. Davis and P. Mermelstein, “Comparison of parametric representations for monosyllabic word recognition in continuously spoken sentences,” *IEEE transactions on acoustics, speech, and signal processing*, vol. 28, no. 4, pp. 357–366, 1980.
- [60] B. Logan *et al.*, “Mel frequency cepstral coefficients for music modeling,” in *Ismir*, vol. 270, no. 1. Plymouth, MA, 2000, p. 11.
- [61] K. Kilgour, M. Zuluaga, D. Roblek, and M. Sharifi, “Fr’echet audio distance: A metric for evaluating music enhancement algorithms,” *arXiv preprint arXiv:1812.08466*, 2018.
- [62] T. Eiter and H. Mannila, *Computing discrete Fréchet distance*. Technical Report CD-TR 94/64, Christian Doppler Laboratory for Expert ..., 1994.
- [63] P. Manocha, Z. Jin, R. Zhang, and A. Finkelstein, “Cdpam: Contrastive learning for perceptual audio similarity,” in *ICASSP 2021-2021 IEEE International Conference on Acoustics, Speech and Signal Processing (ICASSP)*. IEEE, 2021, pp. 196–200.
- [64] D. Jacobellis, D. Cummings, and N. J. Yadwadkar, “Machine perceptual quality: Evaluating the impact of severe lossy compression on audio and image models,” *arXiv preprint arXiv:2401.07957*, 2024.
- [65] J. Hai, H. Wang, D. Yang, K. Thakkar, N. Dehak, and M. Elhilali, “Dpm-tse: A diffusion probabilistic model for target sound extraction,” in *ICASSP 2024-2024 IEEE International Conference on Acoustics, Speech and Signal Processing (ICASSP)*. IEEE, 2024, pp. 1196–1200.
- [66] S. McAdams, S. Winsberg, S. Donnadieu, G. De Soete, and J. Krimphoff, “Perceptual scaling of synthesized musical timbres: Common dimensions, specificities, and latent subject classes,” *Psychological research*, vol. 58, pp. 177–192, 1995.
- [67] S. McAdams, “Musical timbre perception,” *The psychology of music*, vol. 3, 2013.
- [68] S. McAdams and M. Goodchild, “Musical structure: Sound and timbre,” in *The Routledge companion to music cognition*. Routledge, 2017, pp. 129–139.
- [69] H. E. Kemppinen P., “Timbrer: Learning musical timbre transfer in the frequency domain,” Github, 2020. [Online]. Available: <https://github.com/harskish/Timbrer>
- [70] K. J. Piczak, “ESC: Dataset for Environmental Sound Classification,” in *Proceedings of the 23rd Annual ACM Conference on Multimedia*. ACM Press, 2015, pp. 1015–1018. [Online]. Available: <http://dl.acm.org/citation.cfm?doid=2733373.2806390>
- [71] S. Säger, B. Elizalde, D. Borth, C. Schulze, B. Raj, and I. Lane, “Audiopairbank: towards a large-scale tag-pair-based audio content analysis,” *EURASIP Journal on Audio, Speech, and Music Processing*, vol. 2018, pp. 1–12, 2018.
- [72] D.-N. Jiang, L. Lu, H.-J. Zhang, J.-H. Tao, and L.-H. Cai, “Music type classification by spectral contrast feature,” in *Proceedings. IEEE international conference on multimedia and expo*, vol. 1. IEEE, 2002, pp. 113–116.
- [73] M. A. Casey, R. Veltkamp, M. Goto, M. Leman, C. Rhodes, and M. Slaney, “Content-based music information retrieval: Current directions and future challenges,” *Proceedings of the IEEE*, vol. 96, no. 4, pp. 668–696, 2008.